1346 *Biochemistry* **2010,** *49,* 1346–1353
DOI: 10.1021/bi902010t

BIOCHEMISTRY
including biophysical chemistry & molecular biology
Article

Thermodynamic Analysis of a Molecular Chaperone Binding to Unfolded Protein Substrates†

Ying Xu,‡ Sebastian Schmitt,§ Liangjie Tang,‡ Ursula Jakob,*,§ and Michael C. Fitzgerald*,‡

‡*Department of Chemistry, Duke University, Durham, North Carolina 27708, and* §*Department of Molecular, Cellular and Developmental Biology, University of Michigan, Ann Arbor, Michigan 48109*

Received November 23, 2009; Revised Manuscript Received January 12, 2010

ABSTRACT: Molecular chaperones are a highly diverse group of proteins that recognize and bind unfolded proteins to facilitate protein folding and prevent nonspecific protein aggregation. The mechanisms by which chaperones bind their protein substrates have been studied for decades. However, there are few reports about the affinity of molecular chaperones for their unfolded protein substrates. Thus, little is known about the relative binding affinities of different chaperones and about the relative binding affinities of chaperones for different unfolded protein substrates. Here we describe the application of SUPREX (stability of unpurified proteins from rates of H−D exchange), an H−D exchange and MALDI-based technique, in studying the binding interaction between the molecular chaperone Hsp33 and four different unfolded protein substrates, including citrate synthase, lactate dehydrogenase, malate dehydrogenase, and aldolase. The results of our studies suggest that the cooperativity of the Hsp33 folding−unfolding reaction increases upon binding with denatured protein substrates. This is consistent with the burial of significant hydrophobic surface area in Hsp33 when it interacts with its substrate proteins. The SUPREX-derived K_d values for Hsp33 complexes with four different substrates were all found to be within the range of 3−300 nM.

Most proteins must fold into a well-defined three-dimensional structure to carry out their physiological roles within the cell. However, under different kinds of environmental stress conditions, such as elevated temperature, ultraviolet light, exposure of the cell to toxins (e.g., hypochlorous acid, arsenic, or trace metals), and infection, many proteins begin to lose their structure and function. Protein unfolding then often leads to nonspecific aggregation, which is considered to be a largely irreversible process in vivo. Molecular chaperones make up a class of proteins that function in the cell to recognize and selectively bind nonnative proteins to prevent protein aggregation and facilitate their folding. It is generally believed that chaperones interact with unfolding protein substrates via hydrophobic interactions (for a review, see ref *1*). For example, peptide binding studies using a number of different chaperones revealed that most exhibit a greater preference for hydrophobic peptides than for charged, hydrophilic peptides (*2*−*4*). Fluorescent hydrophobic probes have also been used to show that chaperones bind unfolded protein substrates upon exposure of hydrophobic surfaces (*5*−*7*). Finally, analysis of several X-ray crystallographic structures of chaperones indicated they preferentially bind to hydrophobic residues (*4*, *8*, *9*).

While there is an increasing amount of knowledge about the detailed molecular interactions that define chaperone−substrate interactions, much less is known about the binding affinities. The few studies that exist on selected chaperone−substrate complexes have reported binding affinities in the range of 1−170 nM (*10*−*14*). The primary goal of this study is to quantify the binding affinity of the molecular chaperone Hsp33[1] with four different denatured protein substrates, including citrate synthase (CS), lactate dehydrogenase (LDH), malate dehydrogenase (MDH), and aldolase. This work also addresses a fundamental question about molecular chaperone binding interactions, that is whether the binding affinity of a given chaperone for different substrate proteins is the same or different.

Hsp33 is a redox-regulated chaperone holdase from *Escherichia coli*, which prevents HOCl- and other stress-induced protein aggregation both in vitro and in vivo. In its reduced form, Hsp33 is monomeric and inactive. The four conserved cysteine residues, located in the C-terminus of Hsp33, coordinate one zinc ion with very high affinity and constitute the so-called redox-switch domain of Hsp33. Upon oxidative activation of Hsp33, the four cysteine residues form two intramolecular disulfide bridges and release their zinc ion (*15*, *16*). Disulfide bond formation and zinc release induce large conformational rearrangements in Hsp33's C-terminus and cause Hsp33 to adopt a partially unfolded conformation. Two oxidized Hsp33 monomers then dimerize, and Hsp33 acquires its chaperone activity in which one Hsp33 dimer is thought to interact with one unfolded polypeptide substrate (*15*, *17*). Unfolding of Hsp33's C-terminal domain appears to be essential for the exposure

†This work was supported by National Institutes of Health Grant GM065318 to U.J. and National Institutes of Health Grant GM084174 to M.C.F.

*To whom correspondence should be addressed. M.C.F.: Department of Chemistry, Box 90346, Duke University, Durham, NC 27708-0346; telephone, (919) 660-1547; fax, (919) 660-1605; e-mail, michael.c.fitzgerald@duke.edu. U.J.: Department of Molecular, Cellular and Developmental Biology, University of Michigan, Ann Arbor, MI 48109-1048; telephone, (734) 615-1286; fax, (734) 615-1957; e-mail, ujakob@umich.edu.

[1]Abbreviations: Hsp33, heat shock protein 33; $Hsp33_{Ox}$, oxidized heat shock protein 33; CS, citrate synthase; LDH, lactate dehydrogenase; MDH, malate dehydrogenase; H−D exchange, hydrogen−deuterium exchange; SUPREX, stability of unpurified proteins from rates of H/D exchange; GdmCl, guanidine hydrochloride; TFA, triflouroacetic acid; ACN, acetonitrile; MALDI, matrix-assisted laser desorption/ionization; SA, sinapinic acid.

 Published on Web 01/14/2010

of the large hydrophobic surface on the N-terminus of Hsp33, which has been suggested to serve as a binding site for unfolded substrate proteins (*5*).

The experimental strategies employed to date, for evaluating the binding affinities of protein chaperones for their unfolded protein substrates, have involved H−D exchange and NMR-based methods (*12*), fluorescence spectroscopy (*10*, *11*), surface plasmon resonance (*13*), and backscattering interferometry (*14*). Here we utilize an H−D exchange- and mass spectroscopy-based method, termed SUPREX (stability of unpurified proteins from rates of H−D exchange), to measure the binding affinity of Hsp33 for its protein substrates. In SUPREX, the denaturant dependence of the amide H−D exchange reaction is determined to obtain a measure of the thermodynamic parameters associated with the global unfolding−refolding reaction of the protein under study, the Hsp33 protein in this work. The thermodynamic parameters measured in the absence and presence of ligands (the unfolded protein substrates in this work) can ultimately be used to generate thermodynamic information about the binding affinity. The SUPREX technique has been successfully applied to evaluation of the binding affinity of proteins complexed with small molecules (*18*−*21*), peptides (*18*, *21*, *22*), folded proteins (*21*, *23*−*25*), and nucleic acids (*21*, *26*). This study is the first application of SUPREX to the thermodynamic analysis of chaperone-unfolded protein interactions.

EXPERIMENTAL PROCEDURES

Materials. The following reagents were purchased from Sigma-Aldrich (St. Louis, MO): deuterium oxide (99.9% atom D), sodium deuteroxide (35 wt % in D_2O, 99.9% atom D), deuterium chloride (20 wt % in D_2O, 99.5% atom D), sinapinic acid (SA), soybean trypsin inhibitor, and aldolase from rabbit muscle. Guanidine hydrochloride (GdmCl) and trifluoroacetic acid (TFA) were purchased from MP Biochemicals, EMD, and Halocarbon (River Edge, NJ), respectively. Acetonitrile (ACN) was purchased from Fisher (Fair Lawn, NJ), and deuterated phosphoric acid was from Cambridge Isotope Laboratories (Andover, MA). Citrate synthase (CS) from pig heart, malate dehydrogenase (MDH) from pig heart, and lactate dehydrogenase (LDH) from hog muscle were purchased from Roche (Indianapolis, IN).

Protein Expression and Purification. Purification of wild-type Hsp33 and preparation of reduced inactive $Hsp33_{red}$ were conducted as previously described (*5*). To activate Hsp33, 50 μM $Hsp33_{red}$ was incubated with 500 μM NaOCl for 1 h at 30 °C in 40 mM potassium phosphate buffer under constant shaking at 300 rpm. Excess NaOCl was removed using PD-10 desalting columns. The oxidized Hsp33 was concentrated and stored at −80 °C.

Chaperone Activity Measurements. To determine the activity of oxidized Hsp33, light scattering experiments were conducted as previously described (*27*). Briefly, all substrate proteins (CS, MDH, LDH, and aldolase) were incubated in 40 mM HEPES (pH 7.5) in the absence or presence of Hsp33 at concentrations and temperatures as indicated in the figure legends. Light scattering was monitored at λ_{ex} and λ_{em} values of 350 nm using a Hitachi F4500 fluorescence spectrophotometer equipped with a thermostated cuvette holder and stirrer.

Sample Preparation. Concentrated solutions of the substrate proteins CS [376 μM in 50 mM Tris-HCl and 2 mM EDTA (pH 8.0)], MDH [312 μM in 40 mM KH_2PO_4 (pH 7.5)], LDH [457 μM in 40 mM KH_2PO_4 (pH 7.5)], and aldolase (315 μM and 10 mM in ddH_2O) were prepared and centrifuged (13000 rpm for 45 min at 4 °C) to pellet already formed aggregates. The stock concentrations of aldolase and LDH were determined using a Bradford assay (*28*). The concentrations of CS and MDH were determined using their extinction coefficients at 280 nm: 1.78 (*29*) and 0.85 mL mg^{-1} cm^{-1}, respectively (*30*). CS was stored at −80 °C, while MDH, LDH, and aldolase were stored at −20 °C.

A solution of activated Hsp33 (dimeric concentration of 216 μM) was prewarmed in an Eppendorf tube at either 43 °C (for CS), 47 °C (for MDH), 57 °C (for LDH), or 65 °C (for aldolase). Then, concentrated stock solutions of the indicated substrate proteins were added to the activated Hsp33 in a stepwise fashion at the indicated temperatures under constant shaking at 330 rpm, until an Hsp33 dimer:substrate protein ratio of 1:1.5 was reached (final Hsp33 dimer concentration ranging from 114 to 124 μM). During the titration, the solutions remained clear until a molecular ratio of 1:1 (Hsp33 dimer:substrate protein) was reached. Addition of excessive substrate proteins resulted in turbidity due to protein aggregation, indicating that the majority of Hsp33 substrate binding sites is saturated with substrate proteins. These aggregates were removed by centrifugation (13000 rpm for 45 min at 4 °C), and the supernatant was directly used for further experiments.

SUPREX Buffer Preparation. Deuterated GdmCl was used to prepare a series of deuterated H−D exchange buffers containing 40 mM phosphate (pD 7.4) and concentrations of GdmCl ranging from 0.3 to 4 M. The deuterated GdmCl used to prepare the SUPREX buffers was deuterated using four cycles of dissolution in D_2O and lyophilization. The pD of each SUPREX buffer was adjusted with sodium deuteroxide and deuterium chloride. pH measurements were converted to pD measurements via addition of 0.4 to the pH reading (*31*). The final concentrations of GdmCl in the buffers were measured with a refractometer (Bausch and Lomb, Rochester, NY) as described previously (*32*).

Instrumentation. MALDI mass spectra were recorded on an Ultraflex II TOF/TOF mass spectrometer (Bruker Daltonics, Billerica, MA) equipped with a Nd:YAG laser and were the sum of 100 laser shots with the linear and positive mode. The following instrument parameters were used: an ion source 1 voltage of 25 kV, an ion source 2 voltage of 23.4 kV, a lens voltage of 6.8 kV, and a delay time of 600 ns.

SUPREX Data Acquisition and Analysis. A high-sensitivity SUPREX protocol (*33*) was used in this study. Briefly, $Hsp33_{ox}$ and $Hsp33_{ox}$−substrate protein complexes were diluted 10-fold into 10 μL of each GdmCl-containing SUPREX buffer to initiate H−D exchange, which was performed at room temperature. After the specified H−D exchange time at room temperature, the H−D exchange reactions were quenched by addition of TFA to a final concentration of 3% (v/v). A C18 ZipTip (Millipore Corp., Billerica, MA) was used to desalt and concentrate the individual protein samples according to the manufacturer's instructions. The protein was eluted from the ZipTip using 10 μL of a saturated SA-MALDI matrix solution prepared in aqueous buffer containing 45% (v/v) ACN and 0.1% (v/v) TFA. A 1 μL aliquot was placed on a predeposited microcrystalline layer of SA matrix containing aldolase from rabbit muscle and soybean trypsin inhibitor, which were used as the internal mass calibrants.

MALDI-TOF analyses were performed to determine the extent of H−D exchange in each sample. A Microsoft excel macro program script was used to determine the mass-to-charge ratio for the Hsp33 peak. The macro script performed a 19-point

floating average smoothing of the data, a two-point mass calibration using the ion signals from internal mass calibrations, and a center of mass determination for the protein's MALDI ion signal. The extent of deuteration (i.e., Δmass) was calculated for each sample by subtracting the mass of the undeuterated protein from the partially or fully deuterated protein mass. Ten spectra were collected at each denaturant concentration, and the Δmass values derived from these spectra were averaged. The resulting $\Delta mass_{avg}$ values were subsequently plotted against the GdmCl concentration to generate the SUPREX curves (*34*).

The data in each SUPREX curve were fit to a four-parameter sigmoid equation using a nonlinear regression routine in SigmaPlot (Systat Software, Inc., San Jose, CA) to extract a $C^{1/2}{}_{SUPREX}$ value (i.e., concentration of the denaturant at the transition midpoint of the sigmoid curve) from each SUPREX curve. SUPREX curves were collected at several exchange times for Hsp33 and each Hsp33−substrate protein complex. The H−D exchange times used in this work ranged from 2 to 45 min. The $C^{1/2}{}_{SUPREX}$ values determined at the different H−D exchange times were used in eq 1, the derivation of which is described elsewhere (*22*), to determine m and ΔG_f values for Hsp33 in the absence and presence of each substrate protein.

$$-RT\left[\ln\frac{\frac{\langle k_{int}\rangle t}{0.693}-1}{\frac{n^n}{2^{n-1}}[P]^{n-1}}\right] = mC^{1/2}{}_{SUPREX} + \Delta G_f \qquad (1)$$

where R is the gas constant, T is the temperature in kelvin, $\langle k_{int}\rangle$ is the average intrinsic exchange rate of an unprotected amide proton, which is 251 min^{-1}, as calculated using the relationship $\langle k_{int}\rangle = 10^{pH-5}$ min^{-1} (*34*), t is the H−D exchange time, m is defined as $\delta\Delta G_f/\delta$[denaturant], ΔG_f is the folding free energy of the protein in the absence of denaturant, n is the number of protein subunits involved in the folding reaction ($n = 2$ for Hsp33), and [P] is the protein concentration expressed in n-mer equivalents. The left side of the equality in eq 1 will hereafter be termed ΔG_{app}.

Plots of ΔG_{app} versus $C^{1/2}{}_{SUPREX}$ were generated for Hsp33 and each of the protein−substrate complexes. These data were fit to eq 1 using a linear regression routine in Sigma Plot, and the y-intercept and slope were taken to be the ΔG_f and m value (i.e., $\delta\Delta G_f/\delta$[denaturant]), respectively. As described previously (*18*, *19*), we used an averaged m value (m_{avg}) to calculate $\Delta G_{f,avg}$ values. These $\Delta G_{f,avg}$ values were ultimately used to calculate $\Delta\Delta G_{f,avg}$ values for determination of dissociation constants.

In our binding studies of Hsp33, the protein substrates were present in less than a 10-fold excess over the Hsp33 concentration. Therefore, dissociation constants (K_d) were calculated using eq 2 (*35*).

$$K_d = \frac{4L_{total}e^{-\Delta\Delta G_f/NRT} - 4[P]_{total}(e^{-\Delta\Delta G_f/NRT}-1)}{(2e^{-\Delta\Delta G_f/NRT}-1)^2-1} \qquad (2)$$

where L_{total} is the final concentration of ligand in the H−D exchange reaction mixtures, $[P]_{total}$ is the concentration of Hsp33 dimer, $\Delta\Delta G_{f,avg}$ is the difference in $\Delta G_{f,avg}$ between the bound and unbound forms of the protein, and N is the number of independent equivalent binding sites ($N = 1$ as expected for the Hps33 dimer).

RESULTS

Qualitative in Vitro Analysis of Hsp33 Binding Interactions. Hsp33 functions as an ATP-independent molecular chaperone, which binds to a large number of unfolding proteins in vivo as well as to commonly studied chaperone substrate proteins, such as citrate synthase in vitro (*36*). Light scattering experiments were initially conducted to evaluate the ability of activated Hsp33 to inhibit aggregation of thermally unfolding citrate synthase (CS), malate dehydrogenase (MDH), lactate dehydrogenase (LDH), and aldolase. These four proteins differ not only in size, oligomerization status, and isoelectric point but also in the temperature that causes their unfolding and aggregation, which ranges from 43 °C (CS) to 65 °C (aldolase) (Figure 1). To test the influence of $Hsp33_{ox}$ on their thermally induced aggregation, we incubated the enzymes at their respective unfolding temperatures either in the absence or in the presence of a 2-fold molar excess of active $Hsp33_{ox}$ dimers. As shown in Figure 1, the presence of active $Hsp33_{ox}$ suppressed the light scattering of each protein, suggesting that Hsp33 binds the proteins and prevents their irreversible aggregation. These results are consistent with previous observations that activated Hsp33 is a potent chaperone, with wide substrate specificity.

Hsp33's stoichiometry of binding has been previously tested using thermally unfolded luciferase (*37*). The results of these studies suggested that active Hsp33 dimers bind to substrate proteins in a 1:1 stoichiometry. In agreement with these results, we conducted titration experiments in which we titrated increasing concentrations of citrate synthase and the other substrate proteins to a defined concentration of Hsp33 dimers at elevated temperatures (data not shown). No significant aggregation was visible at a 1:1 ratio of Hsp33 dimers to CS monomers. Additional titration of substrate proteins caused visible aggregation, suggesting that the Hsp33 dimer was saturated with substrate protein.

Quantitative in Vitro Analysis of Hsp33 Binding Interactions. The release of protein substrates from Hsp33 appears to require the presence of reducing conditions and a functional DnaK system (*37*). Thus, our preformed complexes between Hsp33 and the substrate proteins were expected to be sufficiently stable at room temperature, which was the temperature at which subsequent SUPREX analyses were performed. Shown in Figure 2 are representative SUPREX curves obtained for Hsp33 alone and Hsp33 complexed with the four different unfolded substrate proteins, CS (Figure 2A), MDH (Figure 2B), aldolase (Figure 2C), and LDH (Figure 2D). The midpoints of the SUPREX transitions (i.e., $C^{1/2}{}_{SUPREX}$) were shifted to a higher denaturant concentration when Hsp33 formed complexes with the substrate proteins (in Figure 2, compare the empty and filled circles). Such a $C^{1/2}{}_{SUPREX}$ shift is consistent with the ligand-induced stabilization of Hsp33.

A total of four SUPREX curves were acquired for each Hsp33−substrate complex using different H−D exchange times that ranged from 2 to 45 min. The $C^{1/2}{}_{SUPREX}$ values for the protein and protein−ligand complexes at the different H−D exchange times are summarized in Table 1. The H−D exchange times in this study were chosen such that they were (i) sufficiently short enough to yield curves with sufficient amplitude to clearly distinguish pretransition baseline values that were distinct and (ii) sufficiently long to yield significant $C^{1/2}{}_{SUPREX}$ value shifts (i.e., greater than 0.1 M). This allowed for accurate determinations of ΔG_f and m values, which involved generating plots of ΔG_{app} versus $C^{1/2}{}_{SUPREX}$ according to eq 1 (Figure 3). Linear least-squares analysis of the data in the resulting plots (Figure 3) indicated that the R^2 values for all the ΔG_{app} versus $C^{1/2}{}_{SUPREX}$ plots were greater than 0.9500−9989 and that the p values

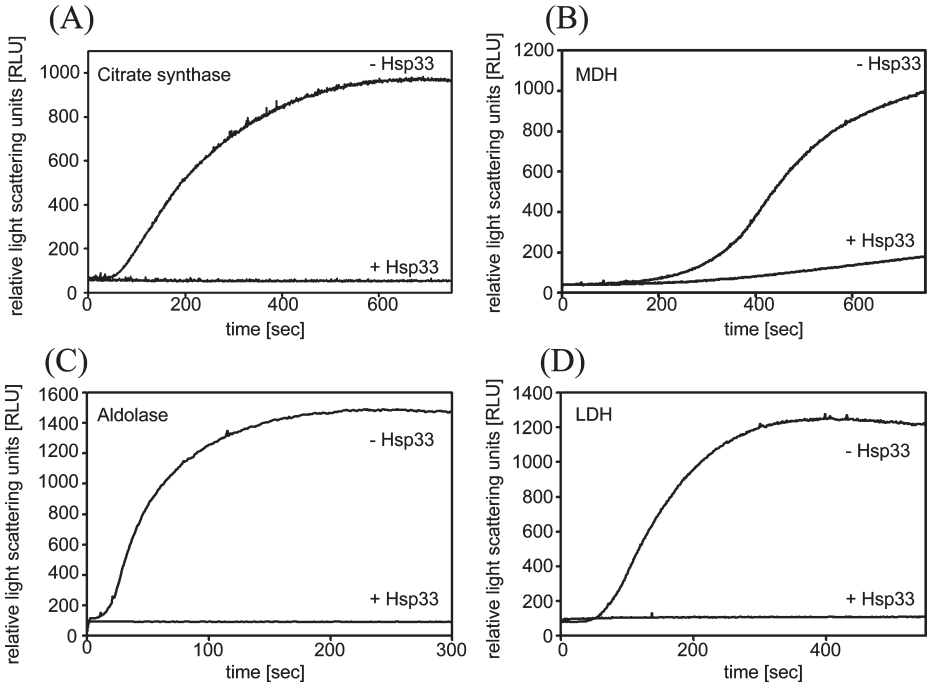

FIGURE 1: Influence of $Hsp33_{ox}$ on thermal protein aggregation in vitro. The purified proteins citrate synthase (final concentration of 170 nM, 43 °C), malate dehydrogenase (final concentration of 120 nM, 47 °C), aldolase (final concentration of 100 nM, 65 °C), and lactate dehydrogenase (final concentration of 150 nM, 55 °C) were incubated in 40 mM HEPES-KOH (pH 7.5) at the respective temperatures in the absence or presence of a 2-fold molar excess of activated $Hsp33_{ox}$ dimers. The concentration of the substrate proteins is given in monomers. Protein aggregate formation of the thermally unfolding proteins was monitored with light scattering measurements.

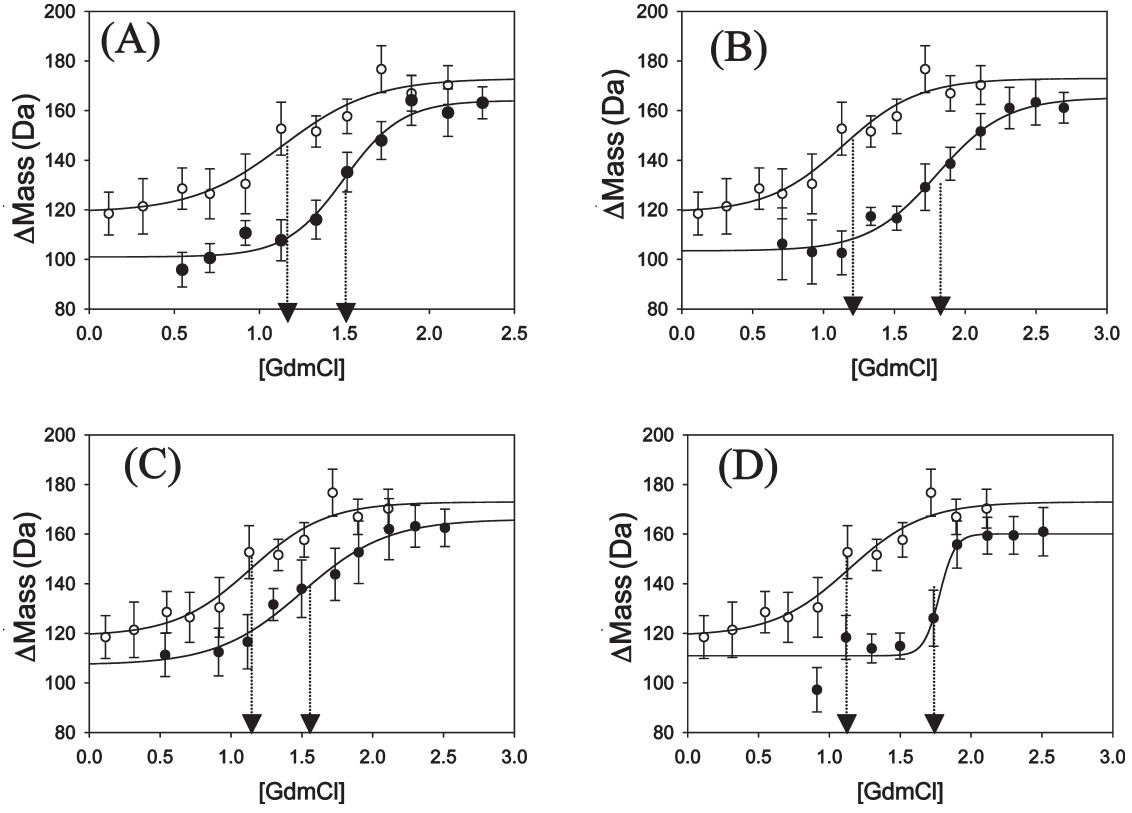

FIGURE 2: Representative SUPREX curves obtained for Hsp33 (○) and its different complexes with (A) CS (●), (B) MDH (●), (C) aldolase (●), and (D) LDH (●). Curves were obtained using the highly sensitive SUPREX protocol in which the H−D exchange time was 15 min. Solid lines are the best fits of the data to a four-parameter sigmoidal equation in SigmaPlot, and the dotted arrows indicate the midpoint ($C^{1/2}_{SUPREX}$) extracted from each SUPREX curve.

ranged from 0.0005 to 0.023. The ΔG_f and m values extracted from each plot of ΔG_{app} versus $C^{1/2}_{SUPREX}$ are summarized in Table 2.

The SUPREX-derived m values for Hsp33 in the presence of the four different protein substrates were all larger than the m value measured for Hsp33 in the absence of the substrate.

Table 1: Transition Midpoints Derived from SUPREX Experiments with Respect to Different H−D Exchange Times for Hsp33 and Its Complexes with Different Protein Substrates

	$C^{1/2}_{SUPREX}$[GdmCl] (M)[a]			
	2 min H−D exchange time	6 min H−D exchange time	15 min H−D exchange time	45 min H−D exchange time
apo-Hsp33	2.1	1.6	1.1	0.8
CS−Hsp33	1.9	1.8	1.5	1.3
MDH−Hsp33	2.4	2.0	1.8	1.5
aldolase−Hsp33	2.3	1.7	1.5	1.3
LDH−Hsp33	2.3	2.0	1.7	1.5

[a]Values are taken from the best fit of the SUPREX curve. Errors were typically between ±0.1 and ±0.2.

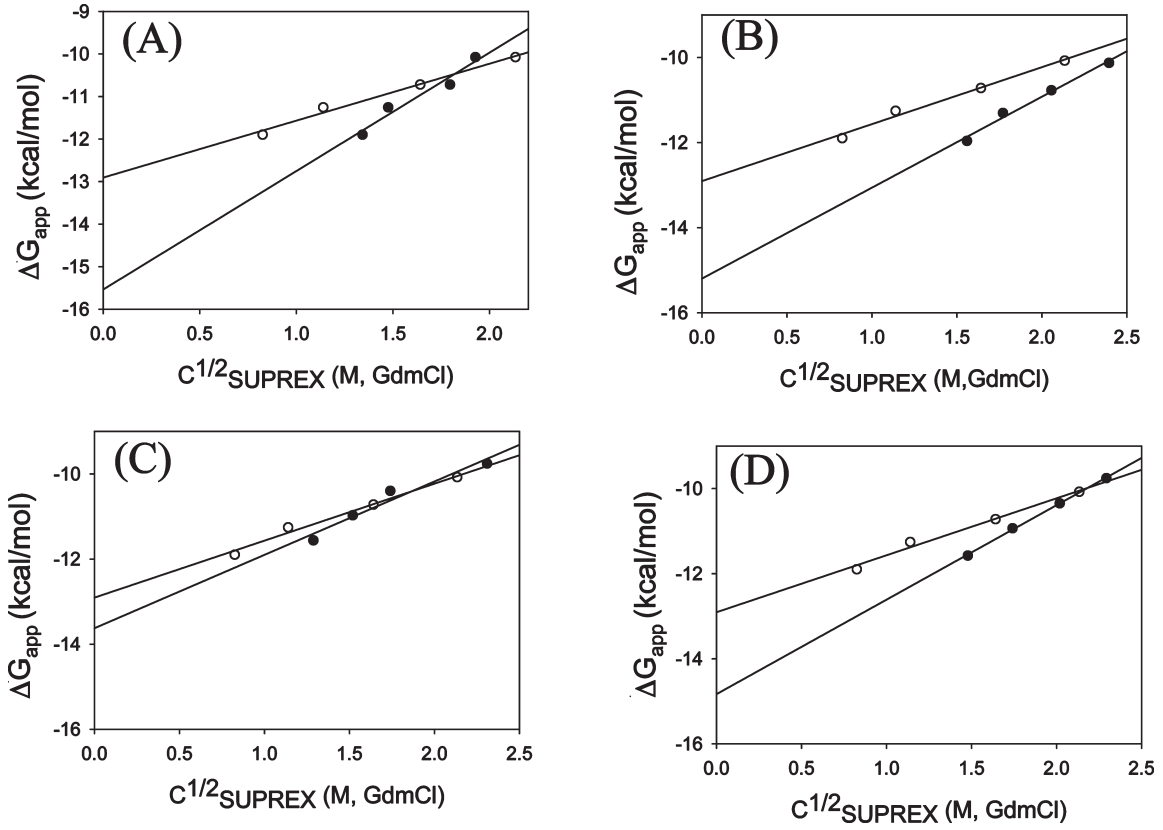

FIGURE 3: Plots of ΔG_{app} vs $C^{1/2}_{SUPREX}$ for Hsp33 (○) and its different complexes with (A) CS (●), (B) MDH (●), (C) aldolase (●), and (D) LDH (●). The resulting *y*-intercept and slope were taken as the ΔG and *m* value, respectively. The H−D exchange time was varied from 2 to 45 min. The solid lines represent the linear least-squares fits of each data set. The R^2 and *p* values obtained in the linear squares analyses ranged from 0.9500 to 0.9989 and from 0.0005 to 0.023, respectively.

Table 2: SUPREX-Derived ΔG_f and *m* Values for Hsp33 and Its Complexes

	ΔG_f[a] (kcal/ mol)	*m*[a] (kcal mol^{-1} M^{-1})	$\Delta G_{f,avg}$[b] (kcal/mol)	m_{avg}[c] (kcal mol^{-1} M^{-1})	$\Delta\Delta G_{f,avg}$ (kcal/mol)	SUPREX- derived K_d (nM)
apo-Hsp33	−12.9 ± 0.2	1.3 ± 0.1	–[d]	–[d]	–	–
CS−Hsp33	−15.5 ± 0.7	2.8 ± 0.4	−14.6 ± 0.2	2.2 ± 0.4	1.7 ± 0.2	30[e] to 302[f]
MDH−Hsp33	−15.2 ± 0.3	2.1 ± 0.2	−15.3 ± 0.1	2.2 ± 0.4	2.4 ± 0.2	3[e] to 82[f]
aldolase−Hsp33	−13.8 ± 0.5	1.8 ± 0.3	−14.5 ± 0.3	2.2 ± 0.4	1.6 ± 0.3	60[e] to 296[f]
LDH−Hsp33	−14.8 ± 0.1	2.2 ± 0.1	−14.8 ± 0.1	2.2 ± 0.4	1.9 ± 0.2	15[e] to 167[f]

[a]The ΔG_f and *m* values were calculated from the linear least-squares analysis of the data using eq 1. The reported errors are the fitting errors of the linear least-squares analyses. [b]$\Delta G_{f,avg}$ values were the average of folding free energy values determined using eq 1 and an established *m* value. The reported errors are the standard deviations of the folding free energy values calculated using eq 1 and the established *m* value. [c]The m_{avg} values were the average of SUPREX-derived *m* values of CS−Hsp33, MDH−Hsp33, LDH−Hsp33, and aldolase−Hsp33 complexes. [d]No m_{avg} value was calculated for apo-Hsp33. [e]K_d values were calculated using eq 2 when the $[Hsp33]_{dimer}$:$[substrate]_{monomer}$ ratio was 1:1. [f]K_d values were calculated using eq 2 when the $[Hsp33]_{dimer}$:$[substrate]_{monomer}$ ratio was 1:1.5.

Application of Peirce's criterion (*38*) to the *m* values in Table 2 confirmed that the apo-Hsp33 *m* value in Table 2 could indeed be considered a statistically significant outlier compared to the other *m* values in Table 2. The increased *m* values obtained for the

Hsp33 complexes imply that the Hsp33 protein folding−unfolding reaction becomes more cooperative in the presence of substrate, which is consistent with the burial of hydrophobic surface area in Hsp33 upon substrate binding. The new hydrophobic surface area that is buried upon substrate binding could be at the binding interface and/or the result of substrate-induced conformational changes at other regions of Hsp33's three-dimensional structure. On the basis of the data of Myers et al. (*39*), the average *m* value increase observed in our experiments, ~1 kcal mol^{-1} M^{-1}, would correspond to a net ~600 Å^2 of hydrophobic surface area being buried in the Hsp33 dimer upon ligand binding.

A quantitative determination of $\Delta\Delta G_f$ values requires an accurate and precise determination of the *m* value. Since the *m* values of four different holo-Hsp33 complexes were determined to be within the experimental error of each other, an average *m* value for Hsp33 in its ligand-bound state was determined from the holo-Hsp33 *m* values listed in Table 2. This average *m* value was used in eq 1 to calculate replicate ΔG_f values directly from the $C^{1/2}_{SUPREX}$ values measured in this work. We have previously shown that this approach can greatly improve the accuracy and precision of ΔG_f values by SUPREX (*18*, *19*). The recalculated ΔG_f values (i.e., the $\Delta G_{f,avg}$ values) are listed in Table 2, along with the $\Delta\Delta G_{f,avg}$ values calculated for each complex.

The $\Delta\Delta G_{f,avg}$ values in Table 2 were used to determine the dissociation constant (i.e., K_d) of each complex (see Table 2). The K_d values in Table 2 are reported as a range because of the uncertainty of the concentration of the protein substrates. As described in Experimental Procedures, the Hsp33 complexes studied in this work were prepared by addition of substrate to a heated Hsp33 solution and then separation of the soluble protein complex from any insoluble substrate aggregates in a centrifugation step. Therefore, it was difficult to calculate the free ligand concentration due to the unknown amount of discarded aggregates. The titration was stopped when the Hsp33 dimer-to-substrate concentration ratio was 1−1.5. Since each polypeptide chain of the unfolded protein substrate is expected to bind to one dimer of the Hsp33 molecule, the total ligand concentration used in the K_d calculations was assumed to be as low as 1 and as high as 1.5 times the Hsp33 dimer concentration. It is noteworthy that only one population of H−D exchanged Hsp33 molecules was detected in the MALDI readout of our SUPREX experiments with Hsp33. This is consistent with the Hsp33 dimer being saturated with protein substrates in our experiments, suggesting that an Hsp33 dimer does indeed bind substrate and that the ligand concentration in our experiments was at least that of the Hsp33 dimer.

DISCUSSION

To obtain accurate ΔG_f and *m* values for a protein folding reaction by SUPREX experiments, the protein under study must (i) have a two-state folding reaction (i.e., protein folding intermediates are not populated, and only the unfolded or folded states of the protein dominate during the folding reaction) and (ii) exhibit EX2 exchange behavior (i.e., the folding reaction must be significantly faster than the intrinsic exchange rate of an unprotected amide proton). To the best of our knowledge, it is unknown whether the folding reaction of Hsp33 is two-state. However, given its relatively large size and multidomain structure, it is unlikely that folding of Hsp33 follows a two-state process. Therefore, the thermodynamic parameters reported here do not represent absolute thermodynamic values for the folding reactions of Hsp33. However, our interest is to measure the difference in folding free energy before and after ligand binding. If it is assumed that the partially folded intermediate state(s) populated in the folding reaction of the apoprotein is the same as those populated in the folding reaction of the holoprotein, then the SUPREX-derived folding free energy values can be used to obtain accurate binding free energies (i.e., $\Delta\Delta G_{f,avg}$ values). Also, if the protein is under non-EX2 (so-called EX1) exchange behavior in our SUPREX experiments, our previous studies demonstrate that the theoretical error introduced into the SUPREX analysis by assuming EX2 exchange was relatively small and can be ignored compared with the experimental error (*40*).

We found that the SUPREX-derived ΔG_f and *m* values for Hsp33 were significantly increased upon ligand binding. The increased ΔG_f values for the Hsp33 complexes with CS, MDH, aldolase, and LDH indicated that Hsp33 binds these unfolded proteins and forms a thermodynamically stable protein−substrate complex. These results are consistent with previous findings that Hsp33−substrate complexes are apparently very stable and require reducing conditions for their dissociation (*37*). The increased *m* values suggest moreover that hydrophobic surface areas in Hsp33 are buried upon ligand binding. Like other heat shock proteins such as GroEL (*41*) and heat shock protein 16.5 (*42*), Hsp33 contains a large hydrophobic surface area located in the N-terminal domain (*43*), which becomes exposed upon the oxidative activation of Hsp33. This N-terminal region has been proposed to serve as the binding site of protein folding intermediates (*43*). In agreement with this hypothesis, we found that formation of a complex of Hsp33 with its denatured protein substrates indeed causes the burial of extensive hydrophobic surface areas, making them much less solvent accessible. This results in a more cooperative folding reaction of the Hsp33 complex. Our SUPREX results (i.e., the increased *m* value) suggest that on the order of 600 Å^2 is buried at the Hsp33−substrate interface. This is a substantial part of the maximum surface area of 3600 Å^2 that has been postulated to potentially serve as the substrate binding site in the Hsp33 dimer (*43*).

Our results suggest that the Hsp33−LDH, Hsp33−aldolase, and Hsp33−CS complexes have K_d values ranging from 15 to 300 nM. The $\Delta\Delta G_{f,avg}$ value obtained for the Hsp33−MDH complex was slightly more negative compared to those of the other three complexes, and the lower bound of the reported K_d range for the Hsp33−MDH complex was approximately 1 order of magnitude smaller compared to the lower bounds of the other three complexes. The lower bound calculation of the K_d value ranges in Table 2 assumes the excess protein substrates in our samples are aggregated and precipitated out of solution prior to our SUPREX analysis. Our light scattering results (Figure 1) suggest that such aggregation and subsequent precipitation are more likely to occur with CS, LDH, and aldolase substrates than with the MDH substrate, as the time course of MDH aggregation is substantially slower than those of the other three substrate proteins. Thus, the K_d values of the Hsp33−LDH, Hsp33−aldolase, and Hsp33−CS complexes are likely to be at the lower end of their reported ranges, whereas the K_d value for the Hsp33−MDH complex is likely to be at the upper end of its reported range, where the K_d calculation assumes no aggregation and precipitation of the unbound protein substrate prior to our SUPREX analysis.

If, as suggested above, we assume that the K_d value of the MDH−Hsp33 complex is near the lower bound reported in Table 2 and the K_d values of the other three complexes are near

the lower bounds reported in Table 2, then the K_d values determined for all the complexes in this work would fall in a range of 15−82 nM. This range is within the range of previously reported binding affinities for other protein folding chaperones binding with their non-native protein substrates. For example, the molecular chaperones GroEL and SecB exhibited a K_d value of 50 nM with denatured Barnase, which was determined using a H−D exchange and NMR-based technique (*12*). Hsp60 was found to have a K_d value of 1.5 nM with denatured recombinant prion protein (*13*). The binding affinities of two closely related small heat shock proteins, an α-crystallin analogue and Hsp27, for a destabilized T4 lysozyme construct have also been reported by fluorescence (*10*, *11*) and back-scattering interferometry (*14*) to be in the range of 1−170 nM.

One major goal of our quantitative thermodynamic studies of Hsp33 and its substrate complexes was to determine if the binding affinities of a given chaperone for different protein substrates were the same or different. Our results obtained for the Hsp33 system suggest that the binding affinities of a given chaperone for a variety of different protein substrates are very similar. These results are quite surprising given that the substrate proteins vary dramatically in their primary amino acid sequence and presumably their state of (un)folding. They raise the intriguing question of the common features that turn these fundamentally different proteins into high-affinity binding partners of chaperone. Analysis of the substrate binding specificity of individual chaperones, such as Hsp33, might shed light on this important problem. Regardless of the detailed molecular features that define the substrate specificity of chaperones, it is interesting to note that the combination of our new data together with existing data strongly suggests that the binding affinities of protein folding chaperones for their denatured protein substrates fall in the low nanomolar range and cluster in a relatively narrow range (i.e., within 1−2 orders of magnitude).

REFERENCES

1. Fink, A. L. (1999) Chaperone-mediated protein folding. *Physiol. Rev. 79*, 425–449.
2. Fenton, W. A., and Horwich, A. L. (1997) GroEL-mediated protein folding. *Protein Sci. 6*, 743–760.
3. Martin, J., and Hartl, F. U. (1997) Chaperone-assisted protein folding. *Curr. Opin. Struct. Biol. 7*, 41–52.
4. Zhu, X. T., Zhao, X., Burkholder, W. F., Gragerov, A., Ogata, C. M., Gottesman, M. E., and Hendrickson, W. A. (1996) Structural analysis of substrate binding by the molecular chaperone DnaK. *Science 272*, 1606–1614.
5. Ilbert, M., Horst, J., Ahrens, S., Winter, J., Graf, P. C. F., Lilie, H., and Jakob, U. (2007) The redox-switch domain of Hsp33 functions as dual stress sensor. *Nat. Struct. Mol. Biol. 14*, 556–563.
6. Wyatt, A. R., Yerbury, J. J., and Wilson, M. R. (2009) Structural Characterization of Clusterin-Chaperone Client Protein Complexes. *J. Biol. Chem. 284*, 21920–21927.
7. Sheluho, D., and Ackerman, S. H. (2001) An accessible hydrophobic surface is a key element of the molecular chaperone action of Atp11p. *J. Biol. Chem. 276*, 39945–39949.
8. Buckle, A. M., Zahn, R., and Fersht, A. R. (1997) A structural model for GroEL-polypeptide recognition. *Proc. Natl. Acad. Sci. U.S.A. 94*, 3571–3575.
9. Kuehn, M. J., Ogg, D. J., Kihlberg, J., Slonim, L. N., Flemmer, K., Bergfors, T., and Hultgren, S. J. (1993) Structural Basis of Pilus Subunit Recognition by the Papd Chaperone. *Science 262*, 1234–1241.
10. Sathish, H. A., Stein, R. A., Yang, G., and McHaourab, H. S. (2003) Mechanism of chaperone function in small heat-shock proteins. Fluorescence studies of the conformations of T4 lysozyme bound to αB-crystallin. *J. Biol. Chem. 278*, 44214–44221.
11. Shashidharamurthy, R., Koteiche, H. A., Dong, J., and McHaourabH. S. (2005) Mechanism of chaperone function in small heat shock proteins: Dissociation of the HSP27 oligomer is required for recognition and binding of destabilized T4 lysozyme. *J. Biol. Chem. 280*, 5281–5289.
12. Zahn, R., Perrett, S., and Fersht, A. R. (1996) Conformational states bound by the molecular chaperones GroEL and SecB: A hidden unfolding (annealing) activity. *J. Mol. Biol. 261*, 43–61.
13. Guerin, M., Bettache, S., Aumelas, A., Chiche, L., and Liautard, J. (2001) Use of surface plasmon resonance to analysis recombinant prion protein interaction with molecular chaperones. *Int. J. Bio-Chromatogr. 6*, 121–131.
14. Latham, J. C., Stein, R. A., Bornhop, D. J., and McHaourab, H. S. (2009) Free-Solution Label-Free Detection of α-Crystallin Chaperone Interactions by Back-Scattering Interferometry. *Anal. Chem. 81*, 1865–1871.
15. Graumann, J., Lilie, H., Tang, X. L., Tucker, K. A., Hoffmann, J. T., Vijayalakshmi, J., Saper, M., Bardwell, J. C. A., and Jakob, U. (2001) Activation of the redox-regulated molecular chaperone Hsp33: A two-step mechanism. *Structure 9*, 377–387.
16. Barbirz, S., Jakob, U., and Glocker, M. O. (2000) Mass spectrometry unravels disulfide bond formation as the mechanism that activates a molecular chaperone. *J. Biol. Chem. 275*, 18759–18766.
17. Graf, P. C. F., Martinez-Yamout, M., VanHaerents, S., Lilie, H., Dyson, H. J., and Jakob, U. (2004) Activation of the redox-regulated chaperone Hsp33 by domain unfolding. *J. Biol. Chem. 279*, 20529–20538.
18. Tang, L., Hopper, E. D., Tong, Y., Sadowsky, J. D., Peterson, K. J., Gellman, S. H., and Fitzgerald, M. C. (2007) H/D exchange- and mass spectrometry-based strategy for the thermodynamic analysis of protein-ligand binding. *Anal. Chem. 79*, 5869–5877.
19. Roulhac, P. L., Powell, K. D., Dhungana, S., Weaver, K. D., Mietzner, T. A., Crumbliss, A. L., and Fitzgerald, M. C. (2004) SUPREX (stability of unpurified proteins from rates of H/D exchange) analysis of the thermodynamics of synergistic anion binding by ferric-binding protein (FbpA), a bacterial transferrin. *Biochemistry 43*, 15767–15774.
20. Wang, M. Z., Shetty, J. T., Howard, B. A., Campa, M. J., Patz, E. F., and Fitzgerald, M. C. (2004) Thermodynamic analysis of cyclosporin A binding to cyclophilin A in a lung tumor tissue lysate. *Anal. Chem. 76*, 4343–4348.
21. Powell, K. D., Ghaemmaghami, S., Wang, M. Z., Ma, L. Y., Oas, T. G., and Fitzgerald, M. C. (2002) A general mass spectrometry-based assay for the quantitation of protein-ligand binding interactions in solution. *J. Am. Chem. Soc. 124*, 10256–10257.
22. Powell, K. D., and Fitzgerald, M. C. (2003) Accuracy and precision of a new H/D exchange- and mass spectrometry-based technique for measuring the thermodynamic properties of protein-peptide complexes. *Biochemistry 42*, 4962–4970.
23. Tong, Y., Wuebbens, M. M., Rajagopalan, K. V., and Fitzgerald, M. C. (2005) Thermodynamic analysis of subunit interactions in *Escherichia coli* molybdopterin synthase. *Biochemistry 44*, 2595–2601.
24. Powell, K. D., Wales, T. E., and Fitzgerald, M. C. (2002) Thermodynamic stability measurements on multimeric proteins using a new H/D exchange- and matrix-assisted laser desorption/ionization (MALDI) mass spectrometry-based method. *Protein Sci. 11*, 841–851.
25. Williams, J. C., Roulhac, P. L., Roy, A. G., Vallee, R. B., Fitzgerald, M. C., and Hendrickson, W. A. (2007) Structural and thermodynamic characterization of a cytoplasmic dynein light chain-intermediate chain complex. *Proc. Natl. Acad. Sci. U.S.A. 104*, 10028–10033.
26. Ma, L., and Fitzgerald, M. C. (2003) A new H/D exchange- and mass spectrometry-based method for thermodynamic analysis of protein-DNA interactions. *Chem. Biol. 10*, 1205–1213.
27. Buchner, J., Grallert, H., and Jakob, U. (1998) Analysis of chaperone function using citrate synthase as nonnative substrate protein. *Methods Enzymol. 290*, 323–338.
28. Bradford, M. M. (1976) Rapid and Sensitive Method for Quantitation of Microgram Quantities of Protein Utilizing Principle of Protein-Dye Binding. *Anal. Biochem. 72*, 248–254.
29. Mcevily, A. J., and Harrison, J. H. (1986) Subunit Equilibria of Porcine Heart Citrate Synthase: Effects of Enzyme Concentration, pH, and Substrates. *J. Biol. Chem. 261*, 2593–2598.
30. Mevarech, M., Eisenberg, H., and Neumann, E. (1977) Malate-Dehydrogenase Isolated from Extremely Halophilic Bacteria of Dead Sea. 1. Purification and Molecular Characterization. *Biochemistry 16*, 3781–3785.
31. Glasoe, P. K., and Long, F. A. (1960) Use of glass electrodes to measure acidities in deuterium oxide. *J. Phys. Chem. 64*, 188–190.
32. Nozaki, Y. (1972) Preparation of guanidine hydrochloride. *Methods Enzymol. 26*, 43–50.
33. Powell, K. D., and Fitzgerald, M. C. (2001) Measurements of protein stability by H/D exchange and matrix-assisted laser desorption ionization mass spectrometry using picomoles of material. *Anal. Chem. 73*, 3300–3304.

34. Ghaemmaghami, S., Fitzgerald, M. C., and Oas, T. G. (2000) A quantitative, high-throughput screen for protein stability. *Proc. Natl. Acad. Sci. U.S.A. 97*, 8296–8301.
35. Segel, I. H. (1975) Enzyme Kinetics, John Wiley & Sons, New York.
36. Jakob, U., Muse, W., Eser, M., and Bardwell, J. C. A. (1999) Chaperone activity with a redox switch. *Cell 96*, 341–352.
37. Hoffmann, J. H., Linke, K., Graf, P. C., Lilie, H., and Jakob, U. (2004) Identification of a redox-regulated chaperone network. *EMBO J. 23*, 160–168.
38. Ross, S. M. (2003) Peirce's criterion for the elimination of suspect experimental data, J. Eng. Technol.
39. Myers, J. K., Pace, C. N., and Scholtz, J. M. (1995) Denaturant M-Values and Heat-Capacity Changes: Relation to Changes in Accessible Surface Areas of Protein Unfolding. *Protein Sci. 4*, 2138–2148.
40. Dai, S. Y., and Fitzgerald, M. C. (2006) Accuracy of SUPREX (stability of unpurified proteins from rates of H/D exchange) and MALDI mass spectrometry-derived protein unfolding free energies determined under non-EX2 exchange conditions. *J. Am. Soc. Mass Spectrom. 17*, 1535–1542.
41. Xu, Z. H., Horwich, A. L., and Sigler, P. B. (1997) The crystal structure of the asymmetric GroEL-GroES-$(ADP)_7$ chaperonin complex. *Nature 388*, 741–750.
42. Kim, K. K., Kim, R., and Kim, S. H. (1998) Crystal structure of a small heat-shock protein. *Nature 394*, 595–599.
43. Kim, S. J., Jeong, D. G., Chi, S. W., Lee, J. S., and Ryu, S. E. (2001) Crystal structure of proteolytic fragments of the redox-sensitive Hsp33 with constitutive chaperone activity. *Nat. Struct. Biol. 8*, 459–466.